

# The triple alpha reaction rate and the $2^+$ resonances in $^{12}\text{C}$

R. de Diego and E. Garrido

*Instituto de Estructura de la Materia, CSIC, Serrano 123, E-28006 Madrid, Spain*

D.V. Fedorov and A.S. Jensen

*Department of Physics and Astronomy, Aarhus University, DK-8000 Aarhus C, Denmark*

(Dated: January 12, 2011)

The triple alpha rate is obtained from the three-body bound and continuum states computed in a large box. The results from this genuine full three-body calculation are compared with standard reference rates obtained by two sequential two-body processes. The fairly good agreement relies on two different assumptions about the lowest  $2^+$  resonance energy. With the same  $2^+$  energy the rates from the full three-body calculation are smaller than those of the standard reference. We discuss the rate dependence on the experimentally unknown  $2^+$  energy. Substantial deviations from previous results appear for temperatures above 3 GK.

PACS numbers: 25.10.+s, 25.40.Lw, 26.30.Hj

*Introduction.* The triple alpha process is the key reaction that permits to bridge the  $A = 5$  and  $A = 8$  gaps, opening the door to the production of  $^{12}\text{C}$  in the core of the stars in the red giant phase [1].

The properties of the  $\alpha$ - $\alpha$ - $\alpha$  continuum states are crucial for the reaction rates, which determine the abundance of  $^{12}\text{C}$  in the Universe. As a clear example, this is what led Fred Hoyle to predict the existence of a  $0^+$  resonance just above the triple  $\alpha$  threshold [2]. It is not possible to explain the observed abundance of  $^{12}\text{C}$  without this so called Hoyle state, which was confirmed experimentally [3] to be at an energy of 0.38 MeV above the three-body threshold. The Hoyle state enhances by itself the reaction rate by about two orders of magnitude at low temperatures (below 2 GK), where the rate is dominated by the electric quadrupole transition from continuum  $3\alpha$   $0^+$  states to the excited bound  $2^+$  state in  $^{12}\text{C}$ .

In type-II supernova explosions dense and hot environments are created. This is the so called hot bubble, consisting of alpha-particles and neutrons, with rather uncertain but relatively high temperature reaching several GK [4]. These environments are the suggested place for the rapid-neutron process [5]. Although the importance of the triple alpha contribution as compared to other reactions in this temperature range ( $T \gtrsim 2$  GK) has been questioned [6], it has also been suggested that changes in this rate imply changes in estimates of the relative amounts of elements formed during the supernovae explosion, and therefore in estimates of the rate at which heavy elements are distributed through the Universe [7]. In [8] the estimated reaction rate for the triple alpha reaction in this temperature range was found to be about an order of magnitude lower than the one given in [9], which would lead to a mass fraction of  $^{56}\text{Ni}$  about two to three times smaller.

At temperatures above 3 GK, the reaction rate for the triple alpha reaction is dominated by the electric quadrupole  $2^+ \rightarrow 0_1^+$  transition [9] (we follow the notation where  $J_i^\pi$  represents the  $i^{\text{th}}$  state in the spectrum with angular momentum  $J$  and parity  $\pi$ . In the partic-

ular case of  $^{12}\text{C}$  the states  $0_1^+$  and  $2_1^+$  are the only ones bound). The reaction rate in this region is therefore to a large extent determined by the properties of the  $2^+$  continuum states, and in particular by the possible existence of a  $2_2^+$  resonance at a relatively low energy. The properties of such a state is still an open problem. The reaction rates given in [9, 10] were computed assuming that  $^{12}\text{C}$  has a  $2_2^+$  resonance at 1.75 MeV. However, in [8] no evidence was found concerning the existence of such  $2^+$  resonance. On the contrary, in [11] an experimental energy of about 2.3 MeV is derived. This value is substantially higher than the one used in [9, 10], and it could substantially modify their computed results. Also, in [12], where a three-body calculation is employed to obtain the resonances as poles of the  $S$ -matrix, a  $2_2^+$  resonance has been found at an energy of 1.38 MeV. However, this energy is found with the same (adjustable) three-body interaction that reproduces the energy of the bound  $2_1^+$  state.

The role of the  $2_2^+$  resonance in  $^{12}\text{C}$  in the triple alpha reaction rate requires detailed investigation. We shall employ the same three-body method as in [13], where no assumption is made about the capture mechanism (sequential or direct), and in contrast to the method described in [9], where a sequential capture process is assumed. The standard procedure and the almost canonical results of [9] is furthermore tested by comparison.

*Full three-body formulation.* The first of the methods used in this work is the three-body calculation described in [13]. Let us consider the radiative capture process  $a + b + c \rightarrow A + \gamma$ , where  $A$  is a bound system made of particles  $a$ ,  $b$ , and  $c$  with separation energy  $B_A$ . The corresponding reaction rate  $R_{abc}(E)$  is given by [13, 14]

$$R_{abc}(E) = \frac{\hbar^3}{c^2} \frac{8\pi}{(\mu_x \mu_y)^{3/2}} \left( \frac{E_\gamma}{E} \right)^2 \frac{2g_A}{g_a g_b g_c} \sigma_\gamma(E_\gamma) \quad (1)$$

where  $E = E_\gamma + B_A$  is the initial three-body kinetic energy,  $E_\gamma$  is the photon energy,  $\sigma_\gamma(E_\gamma)$  is the photo dissociation cross section of the  $A$  nucleus,  $c$  is the velocity of light,  $g_i$  is the spin degeneracy of states of particle

$i = a, b, c, A$ , and  $\mu_x$  and  $\mu_y$  are the reduced masses of the systems related to the Jacobi coordinates,  $(\mathbf{x}, \mathbf{y})$ , for the three-body system [15].

The photo dissociation cross section for the inverse process  $A + \gamma \rightarrow a + b + c$  can be expanded into electric and magnetic multipoles. In particular, the electric multipole contribution of order  $\lambda$  has the form [13]:

$$\sigma_\gamma^{(\lambda)}(E_\gamma) = \frac{(2\pi)^3(\lambda+1)}{\lambda[(2\lambda+1)!!]^2} \left(\frac{E_\gamma}{\hbar c}\right)^{2\lambda-1} \frac{d\mathcal{B}}{dE}, \quad (2)$$

where the strength function  $\mathcal{B}$  is

$$\mathcal{B}(E\lambda, n_0 J_0 \rightarrow nJ) = \sum_{\mu M} |\langle nJM | O_\mu^\lambda | n_0 J_0 M_0 \rangle|^2, \quad (3)$$

where  $J_0$ ,  $J$  and  $M_0$ ,  $M$  are the total angular momenta and their projections of the initial and final states, and all other quantum numbers are collected into  $n_0$  and  $n$ . The electric multipole operator is given by:

$$O_\mu^\lambda = \sum_{i=1}^3 z_i |\mathbf{r}_i - \mathbf{R}|^\lambda Y_{\lambda,\mu}(\Omega_{y_i}), \quad (4)$$

where  $i$  runs over the three particles of charges  $z_i$ , and where we neglect contributions from intrinsic transitions within each of the three constituents [16].

Finally the energy averaged reaction rate is obtained as a function of the temperature by using the Maxwell-Boltzmann distribution as weighting function. For three alpha particles we obtain [13]:

$$\begin{aligned} \langle R_{\alpha\alpha\alpha}(E) \rangle &= \frac{\hbar^3}{c^2} \frac{48\pi}{(\mu_{\alpha\alpha}\mu_{\alpha^8\text{Be}})^{3/2}} (2J+1) e^{-\frac{E}{k_B T}} \times \\ &\times \frac{1}{(k_B T)^3} \int_{|B|}^\infty E_\gamma^2 \sigma_\gamma^{(\lambda)}(E_\gamma) e^{-\frac{E_\gamma}{k_B T}} dE_\gamma, \end{aligned} \quad (5)$$

where  $k_B$  is the Boltzmann constant.

The strength function  $\mathcal{B}$  is computed by genuine three-body calculations of both the bound final state,  $|n_0 J_0 M_0\rangle$ , and the continuum initial states,  $|nJM\rangle$ . We use the hyperspherical adiabatic expansion method described in [15]. The  $\alpha$ - $\alpha$  interaction is given in [17]. The basic procedure is computation of three-body states of given angular momentum and parity confined by box boundary conditions [18]. In this way the continuum spectrum is discretized. The strength functions are then obtained for each discrete continuum state according to Eq.(3). The distribution  $d\mathcal{B}/dE$  is built by use of the finite energy interval approximation, where the energy range is divided into bins, and all the discrete values of  $\mathcal{B}$  falling into a given bin are added. Afterwards the points are connected by spline operations and the expressions (2) and (5) are computed.

*Sequential process.* The NACRE results given in [9] are usually taken as the reference for the reaction rates in the triple alpha process. In this work the process is assumed to proceed in a sequentially two-step process.

In the first step one  $\alpha$ -particle captures another one to produce  $^8\text{Be}$  in the ground  $0^+$  resonant state. In the second step,  $^8\text{Be}$  is able to capture (before decaying) a third  $\alpha$ -particle, populate a  $^{12}\text{C}$  resonance, and then decay by photo emission to one of the bound states of  $^{12}\text{C}$ . The reaction rate for such a two-step process is given by the rate for the capture of an  $\alpha$ -particle by  $^8\text{Be}$  ( $\langle R_{\alpha^8\text{Be}}(E'', E') \rangle$ ) weighted with the rate for formation of  $^8\text{Be}$  [9]:

$$\begin{aligned} \langle R_{\alpha\alpha\alpha}(E') \rangle &= 3 \frac{8\pi\hbar}{\mu_{\alpha\alpha}^2} \left( \frac{\mu_{\alpha\alpha}}{2\pi k_B T} \right)^{3/2} \\ &\int_0^\infty \frac{\sigma_{\alpha\alpha}(E'')}{\Gamma_\alpha(^8\text{Be}, E'')} e^{-E''/k_B T} \langle R_{\alpha^8\text{Be}}(E'', E') \rangle E'' dE'', \end{aligned} \quad (6)$$

where  $E''$  and  $E'$  are the relative energy between the two  $\alpha$ -particles forming  $^8\text{Be}$  and the energy of the third  $\alpha$ -particle relative to the center of mass of the first two, respectively. The temperature is  $T$  and  $\mu_{\alpha\alpha}$  is the reduced mass of the two-alpha system. The elastic  $\alpha - \alpha$  cross section is given by:

$$\sigma_{\alpha\alpha}(E'') = \frac{2\pi}{\kappa^2} \frac{\Gamma_\alpha(^8\text{Be}, E'')^2}{(E'' - E_r)^2 + (\Gamma_\alpha(^8\text{Be}, E''))^2/4}, \quad (7)$$

where  $\kappa^2 = 2\mu_{\alpha\alpha}E''/\hbar^2$ ,  $E_r$  is the  $^8\text{Be}$  resonance energy, and the width  $\Gamma_\alpha(^8\text{Be}, E'')$  has the form [9]:

$$\Gamma_\alpha(^8\text{Be}, E'') = \Gamma_\alpha \frac{P_\ell(E'')}{P_\ell(E_r)}, \quad (8)$$

where  $\Gamma_\alpha$  is the width of the resonance,  $P_\ell$  is the penetration factor, and  $\ell$  is the relative orbital angular momentum between the two  $\alpha$ -particles.

In our case, the experimental energy of the  $0^+$  resonance in  $^8\text{Be}$  is  $E_r = 0.09189$  MeV above threshold, with a width of  $\Gamma_\alpha = 6.8 \pm 1.7 \cdot 10^{-6}$  MeV. For such a narrow resonance we have that  $\Gamma_\alpha(^8\text{Be}, E'') \approx \Gamma_\alpha$ , and for our purpose we can safely replace Eq.(7) by:

$$\frac{\sigma_{\alpha\alpha}(E'')}{\Gamma_\alpha(^8\text{Be}, E'')} = \frac{4\pi^2}{\kappa^2} \delta(E'' - E_r), \quad (9)$$

from which Eq.(6) becomes:

$$\begin{aligned} \langle R_{\alpha\alpha\alpha}(E') \rangle &= 3 \frac{8\pi\hbar}{\mu_{\alpha\alpha}^2} \left( \frac{\mu_{\alpha\alpha}}{2\pi k_B T} \right)^{3/2} \\ &\times \frac{4\pi^2}{\kappa^2} E_r e^{-E_r/k_B T} \langle R_{\alpha^8\text{Be}}(E') \rangle \end{aligned} \quad (10)$$

Finally, from Ref.[9] we have:

$$\begin{aligned} \langle R_{\alpha^8\text{Be}}(E') \rangle &= \frac{8\pi}{\mu_{\alpha^8\text{Be}}^2} \left( \frac{\mu_{\alpha^8\text{Be}}}{2\pi k_B T} \right)^{3/2} \\ &\times \int_0^\infty \sigma_{\alpha^8\text{Be}}(E') e^{-E'/k_B T} E' dE', \end{aligned} \quad (11)$$

where

$$\begin{aligned} \sigma_{\alpha^8\text{Be}}(E') &= \sum_{J=0,2} (2J+1) \frac{\pi\hbar^2}{2\mu_{\alpha^8\text{Be}} E'} \\ &\times \frac{\Gamma_\alpha(^{12}\text{C}^J, E') \Gamma_\gamma(^{12}\text{C}^J, E')}{(E' - E_r^J)^2 + 0.25\Gamma(^{12}\text{C}^J, E')^2} \end{aligned} \quad (12)$$

	$E_r^J$	$\Gamma_\alpha(^{12}\text{C}^J)$	$\Gamma_\gamma(^{12}\text{C}^J)$	$E_T^J$
$J = 0$	0.2877	$8.3 \cdot 10^{-6}$	$3.7 \cdot 10^{-9}$	2.928
$J = 2$	1.75	0.56	$0.2 \cdot 10^{-6}$	7.367

TABLE I: Values of the parameters entering in Eqs.(12) to (15) taken from Ref.[9]. They are all given in MeV.

where  $E_r^J$  is the  $^{12}\text{C}$  resonance energy with angular momentum  $J$ , and

$$\Gamma(^{12}\text{C}^J, E') = \Gamma_\alpha(^{12}\text{C}^J, E') + \Gamma_\gamma(^{12}\text{C}^J, E') \quad (13)$$

$$\Gamma_\alpha(^{12}\text{C}^J, E') = \Gamma_\alpha(^{12}\text{C}^J) \frac{P_\ell(E')}{P_\ell(E_r^J)} \quad (14)$$

$$\Gamma_\gamma(^{12}\text{C}^J, E') = \Gamma_\gamma(^{12}\text{C}^J) \frac{(E_T^J + E')^5}{(E_T^J + E_r^J)^5} \quad (15)$$

The parameters needed to compute Eq.(12), and therefore (11) and (10), are taken from [9] and they are collected in table I.

Given a transition between  $^{12}\text{C}$  continuum states with angular momentum  $J$  and a bound  $^{12}\text{C}$  state with binding energy  $B_J$ , it is now possible to extract the expression for  $d\mathcal{B}/dE$  effectively used in Ref.[9]. This can be made by inserting Eq.(11) into (10), and Eq.(2) with  $\lambda=2$  into Eq.(5). By comparison of those expressions we extract:

$$\frac{d\mathcal{B}}{dE} = \frac{1}{\alpha} \frac{375}{8\pi^2} \frac{(\hbar c)^4}{(E + |B_J|)^5} \frac{\Gamma_\alpha(^{12}\text{C}^J, E') \Gamma_\gamma(^{12}\text{C}^J, E')}{(E' - E_r^J)^2 + 0.25 \Gamma(^{12}\text{C}^J, E')^2}, \quad (16)$$

where  $E = E_r + E'$  is the three-body kinetic energy and  $\alpha$  is the fine structure constant.

*Comparing the methods.* In [13] the full three-body method was used to compute the reaction rate for the triple  $\alpha$  process. The  $\alpha$ - $\alpha$  interaction in [17] was used. This leads to the  $^{12}\text{C}$  spectrum given in [12], which results in good agreement with the experimental data for about 13 different states. In particular, concerning the  $2^+$  resonances, the computed  $^{12}\text{C}$  spectrum includes a low lying one at 1.38 MeV (above the three-body threshold) with a computed width of 0.13 MeV, and a second one at 4.4 MeV with a width of about 1 MeV. Experimentally only a resonance at 3.88 MeV is fully established. In Ref.[12] the resonances are obtained as poles of the  $S$ -matrix by use of the complex scaling method [19]. With this method the resonances behave asymptotically as bound states with complex energy, which automatically determines the resonance energy and the corresponding width. The resonance width is then not a parameter but an output of the calculation. The three-body calculation, as described in [13], gives rise to the triple  $\alpha$  reaction rate shown by the thick solid line in Fig.1. The contributions coming from the  $0^+ \rightarrow 2_1^+$  and  $2^+ \rightarrow 0_1^+$  transitions are shown by the corresponding thin solid lines. The agreement between the total reaction rate and the result given in [9]

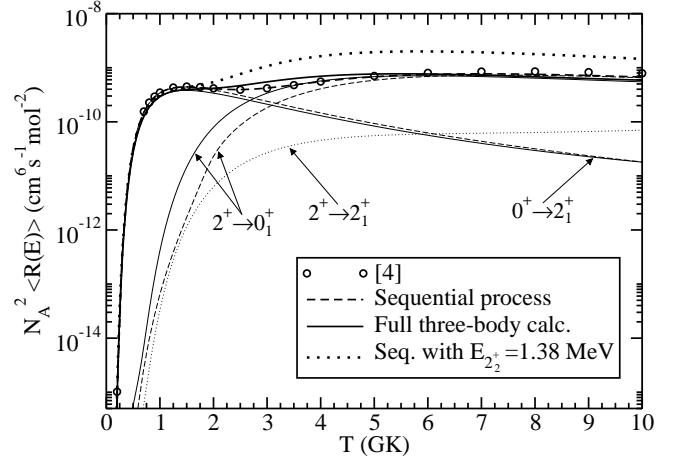


FIG. 1: Reaction rate for the triple  $\alpha$  process with the full three-body calculation (thick solid line) and the sequential approach (thick dashed line) as described in the text. The corresponding contributions from the  $0^+ \rightarrow 2_1^+$  and  $2^+ \rightarrow 0_1^+$  transitions are given by the thin curves ( $2_1^+$  and  $0_1^+$  refer to the lowest  $2^+$  and  $0^+$  states in the  $^{12}\text{C}$  spectrum, which are the only ones bound). The thin dotted line is the contribution from the  $2^+ \rightarrow 2_1^+$  in the full three-body calculation. The open circles correspond the rate given in [9]. The thick dotted curve is a sequential calculation but using the same energy and width for the  $2_2^+$  resonance as in the three-body calculation.

(open circles in the figure) is reasonably good. For completeness, we show in the figure the contribution from the  $2^+ \rightarrow 2_1^+$  transition (thin dotted curve). This contribution is very small and could actually be neglected.

When the sequential approach is used, and the reaction rate is obtained from Eq.(10), we get the thick dashed curve in the figure. The sequential method described in the present work and in [9] are identical except for the approximation in Eq.(9). The parameters used in the calculations (table I) are also the same in both cases. The good agreement between the thick dashed curve and the circles in Fig.1 shows that the approximation in Eq.(9) is accurate. Only a small difference is found for high temperatures since the contribution from the  $3_1^-$  resonance in  $^{12}\text{C}$  is included in [9], but completely neglected in our calculation. Again, the corresponding thin dashed lines show the contributions to the total rate from the  $0^+ \rightarrow 2_1^+$  and  $2^+ \rightarrow 0_1^+$  transitions.

As seen in Fig.1, the contribution from the  $0^+ \rightarrow 2_1^+$  transition is very similar in the full three-body calculation and the sequential approximation. This is due to the narrow  $0_2^+$  Hoyle three-body state in  $^{12}\text{C}$  which heavily dominates the full calculation. It has a large strength corresponding to strong population and subsequent decay into the bound  $2_1^+$  state plus a photon. This process is precisely as assumed in the sequential description, and in fact the reason for its success.

However, the lowest  $2_2^+$  resonance in  $^{12}\text{C}$  (both the one obtained in the three-body calculation and the one used

in [9]) is rather wide, which means that the continuum non-resonant three-body  $2^+$  states can contribute significantly to the  $2^+ \rightarrow 0_1^+$  transition. In fact, as seen in the figure, the three-body and the sequential calculation differ for this contribution, especially at low temperatures. Due to this discrepancy the two computed total reaction rates do not fully agree for temperatures from about 2 to 5 GK. When the temperature increases the thin solid and thin dashed curves in Fig.1 become closer and closer, in such a way that for temperatures higher than 5 GK the total reaction rate is similar in both calculations.

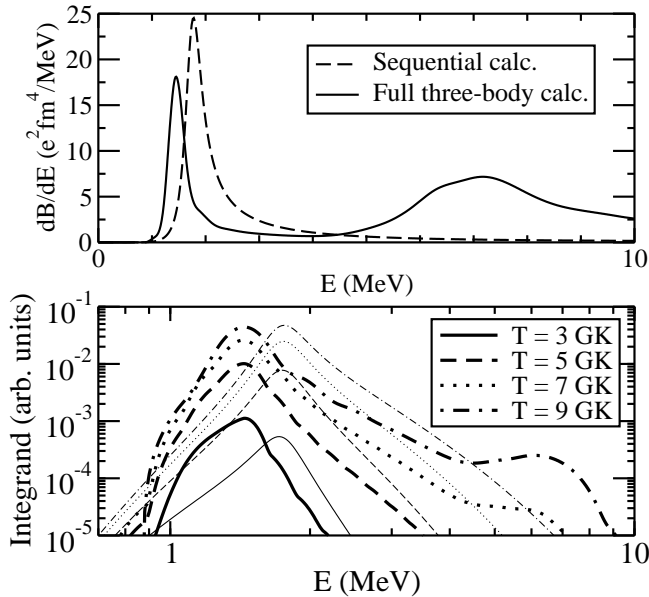


FIG. 2: Upper part: the  $dB/dE$  function for the  $2^+ \rightarrow 0_1^+$  transition for the sequential approach as given in Eq.(16) (dashed curve) and the three-body calculation (solid curve). Lower part: Integrands of Eq.(5) (thick curves) and Eq.(10) (thin curves) in arbitrary units as a function of the kinetic energy of the three  $\alpha$ 's for  $T=3, 5, 7$ , and  $9$  GK. The thick lines and thin lines correspond to the full three-body and the sequential calculations, respectively.

The fact that both calculations produce basically the same result is encouraging. However, this good agreement is apparently inconsistent, since it is achieved in spite of different energies of the lowest  $2_2^+$  resonance in  $^{12}\text{C}$ . While in the full three-body calculation this energy is  $1.38$  MeV, the sequential result is computed for an energy of  $1.75$  MeV. In fact, when the sequential calculation is performed using the same energy ( $1.38$  MeV) and width ( $0.13$  MeV) as in the full three-body calculation we obtain the rate given by the thick dotted curve in Fig.1. As we can see, for the same parameters in the low-lying  $2_2^+$  resonance in  $^{12}\text{C}$ , the sequential calculation gives a rate that, for temperatures beyond  $2$  GK, is clearly above the one obtained in the three-body calculation.

For a better understanding it is useful to compare the  $dB/dE$  function for the  $2^+ \rightarrow 0_1^+$  transition obtained in the full three-body calculation and in the sequen-

tial approximation from Eq.(16). This comparison is shown in the upper part of Fig.2 by the solid and dashed curves, respectively. The  $dB/dE$  function in the sequential case is essentially a lorentzian centered around the  $1.75$  MeV corresponding to the  $2_2^+$  resonance energy. In the full three-body calculation the peak, as expected, is located at about  $1.4$  MeV. Furthermore, a shoulder appears for higher energies arising from the contribution from continuum non-resonant states and the additional  $2^+$  resonances obtained in the three-body calculation. These contributions are not included in the description in Ref.[9].

However, due to the exponentials in Eq.(5) or (11), the high energy region of the transition strength contributes very little to the reaction rate. This is shown in the lower part of the figure, where we plot the integrands entering in the calculation of the reaction rate (Eqs.(5) and (10)) as a function of the three-body kinetic energy for  $T=3, 5, 7$ , and  $9$  GK. The thick and thin curves correspond to the full three-body and the sequential calculations, respectively. As expected, these integrands die rather fast with the energy, and the larger the temperature the larger the energy range contributing to the reaction rate.

As seen in the upper part of the figure, the full three-body calculation accumulates part of the strength at smaller energies than the sequential calculation. This is first of all due to the different resonance energies of  $1.38$  MeV in the three-body and  $1.75$  MeV in the sequential calculation. For this reason, for low temperatures, i.e. for  $T \leq 3$  GK, where the integrand is vanishingly small for  $E \gtrsim 2$  MeV (see the solid curves in the lower part of the figure), the three-body calculation provides a higher reaction rate than in the sequential approximation. The integral of the thick solid line in the lower part of Fig.2 is almost twice the one of the thin solid curve. When the temperature increases, the energy at which the integrand begins to vanish also increases, and the sequential reaction rate adds more strength compared to the three-body case. As a consequence both reaction rates approach each other, and they even cross at some point. The integral of the thin dot-dashed curve in the lower part of Fig.2 (sequential case for  $T=9$  GK) is about 25% bigger than the one of the thick dot-dashed curve (three-body case for  $T=9$  GK). Even for  $T = 9$  GK the integrand only allows contribution up to energies around  $5$  MeV, which means that the behavior of the  $dB/dE$  function for  $E \gtrsim 5$  MeV is rather unimportant.

Thus, from Fig.2 we can conclude that the full three-body calculation shifts part of the strength to large energies, which contribute very little to the reaction rate. For this reason, for the same low lying  $2_2^+$  resonance energy in  $^{12}\text{C}$ , the full three-body calculation provides a smaller rate than the sequential calculation. Or, in other words, for the three-body and sequential calculations to provide the same reaction rate, the  $2_2^+$  resonance energy has to be smaller in the three-body case, in order to compensate the non-contributing part of the strength at large energies (for instance  $1.38$  MeV in the three-body calculation

and 1.75 MeV in the sequential approach).

*The  $2_2^+$  resonance energy and the reaction rate.* As seen in Fig.1, for temperatures below about 3 GK the reaction rate of the triple  $\alpha$  reaction is dominated by the  $0^+ \rightarrow 2_1^+$  transition, and the precise energy of the lowest  $2_2^+$  resonance in  $^{12}\text{C}$  does not play any role. Only for temperatures beyond 4 GK the energy of the  $2_2^+$  resonance has a sizable effect.

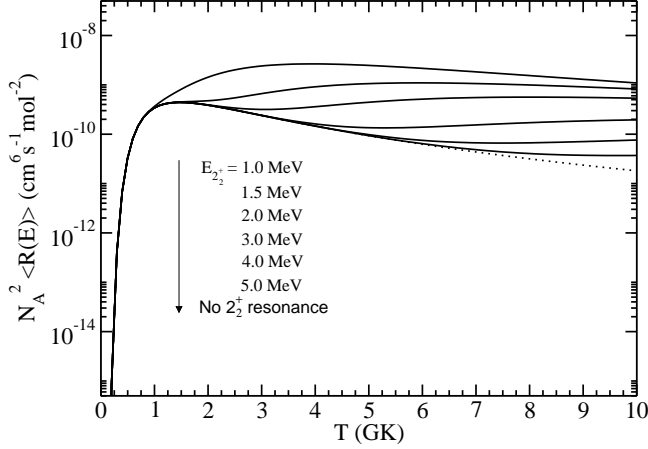


FIG. 3: Reaction rate in the sequential case for different energies of the lowest  $2_2^+$  resonance in  $^{12}\text{C}$ . The energy increases from the upper curve to the lower one from 1 MeV up to 5 MeV. The dotted curve is the calculation where the contribution from the  $2^+ \rightarrow 0_1^+$  transition has been completely removed.

Fig.3 shows the total sequential reaction rate for different energies of the  $2_2^+$  resonance in  $^{12}\text{C}$ . The rate decreases progressively when the resonance is placed at a higher and higher energy. This happens because the higher the energy of the  $2_2^+$  resonance, the more strength located at high three-body energies, where the integrand is small due to the exponential in Eq.(5) or (11) (see the lower part of Fig.2). In fact, for a resonance energy of 5 MeV the computed rate is quite similar to the one obtained when the resonance is removed. Only for temperatures beyond around 7 GK some difference appears.

For the same reason, the same behavior is found for the three-body calculation. An increase of the  $2_2^+$  resonance energy decreases the reaction rate. However, full removal of the  $2_2^+$  resonance in  $^{12}\text{C}$  gives a rate that differs quite a lot from the one obtained when the full contribution from the  $2^+ \rightarrow 0_1^+$  transition is removed. This can be seen in Fig.4, where the thick solid line is the same calculation as in Fig.1 (with the  $2_2^+$  resonance at 1.38 MeV), the thick dashed line is the calculation after removal of this  $2_2^+$  resonance, and the thin solid line is the result when the full  $2^+ \rightarrow 0_1^+$  transition is excluded. The difference between the thin solid line and the thick dashed line in the figure shows the importance of including the additional continuum  $2^+$  states in  $^{12}\text{C}$ .

It is important to keep in mind that the three-body calculation, together with the  $2_2^+$  resonance at 1.38 MeV,

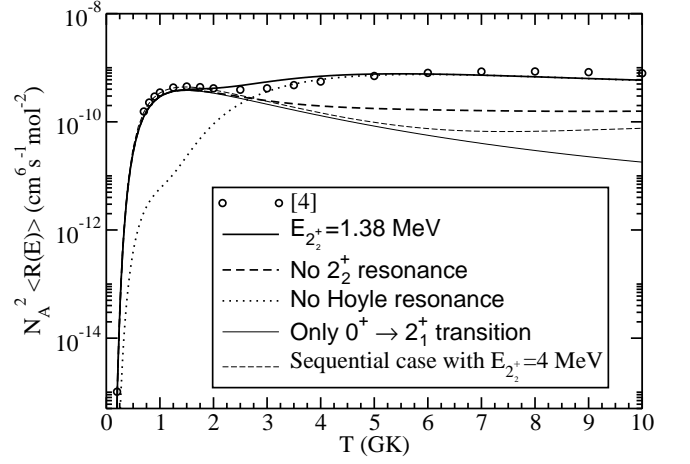


FIG. 4: Reaction rate for the three-body calculation when the  $2_2^+$  resonance is placed at 1.38 MeV (thick solid line), when the resonance is removed from the calculation (thick dashed line), when the full contribution from the  $2^+ \rightarrow 0_1^+$  transition is excluded (thin solid line), and when the Hoyle resonance is removed (dotted line). The thin dashed curve is the calculation in the sequential case when the energy of the  $2_2^+$  resonance is 4.0 MeV. The open circles are taken from [9].

includes as well all the other states obtained in [12], in particular the  $2_3^+$  resonance around 4 MeV. For this reason, the thick dashed line in Fig.4, where the resonance at 1.38 MeV has been suppressed, still contains the contribution of the one at about 4 MeV, which is the one experimentally known. Then the thick dashed line in the figure gives a lower limit to the triple  $\alpha$  reaction rate, since this is what we would get in case that the  $2^+$  resonance in  $^{12}\text{C}$  around 1.5-2.5 MeV is shown not to exist.

In this connection it is interesting to compare the thick dashed line in the figure with the thin dashed line, which represents the reaction rate obtained in the sequential approach when the lowest  $2_2^+$  resonance in  $^{12}\text{C}$  is placed at 4.0 MeV. This is very close to the energy of the lowest  $2_2^+$  resonance fully confirmed experimentally, and therefore this would be what provided by the sequential calculation in case that the  $2^+$  resonance in  $^{12}\text{C}$  around 1.5-2.5 MeV does not exist. The difference between both dashed curves shows the effect of the non-resonant  $2^+$  states in this case.

For illustration we also show in Fig.4 the reaction rate that we obtain when the Hoyle resonance is removed from the calculation (dotted curve in the figure). As we can see, this state is responsible for an increase of the reaction of about two orders of magnitude for temperatures below 3 GK.

Thus, from Fig.4 we can conclude that in case that the low-lying  $2_2^+$  resonance is confirmed not to exist (such that the lowest one is the already known resonance close to 4 MeV above threshold) the sequential approach would underestimate the triple- $\alpha$  reaction rate. The non-resonant  $2^+$  states in  $^{12}\text{C}$  are enough to increase significantly the rate at high temperatures.

*Summary and conclusions.* We investigate the reaction rate for the triple  $\alpha$  reaction. We used the full three-body calculation described in [13] and the sequential description of [9]. For the same set of three-body resonances we find that the full three-body calculation gives smaller rates than the sequential approximation for temperatures above  $\sim 3$  GK.

We focus on the importance of the experimentally uncertain lowest  $2_2^+$  resonance in  $^{12}\text{C}$  which to a large extent determines the reaction rate for temperatures above 3 GK. Different theoretical calculations predict a  $2_2^+$  resonance in  $^{12}\text{C}$  at around 1.0-2.5 MeV. We find that when the full and sequential calculations are performed taking a  $2_2^+$  resonance energy of 1.38 MeV and 1.75 MeV, respectively, the computed total reaction rates are quite similar for the whole range temperature. The only exception is for temperatures ranging between about 2 and 5 GK, where the full calculation gives a rate slightly above the one obtained with the sequential calculation. The reason for this behavior is that part of the strength in the three-body case is moved to higher energies due to the higher  $2^+$  resonances and non-resonant continuum  $2^+$  states. The high energy part of this strength contributes very little, and the missing low-energy strength has to be compensated by a lower-lying  $2^+$  resonance. For the same energy and width of the  $2_2^+$  resonance, the full three-body calculation contributes less than the sequential approximation.

If the lowest  $2_2^+$  resonance in  $^{12}\text{C}$  by chance should be at about 4 MeV, where the lowest established  $2^+$  state is located, then the reaction rate is higher for the full three-body calculation than obtained from the sequential approximation. This is due to contributions from the non-resonant continuum states in the three-body calculation and the insignificant contribution from a high-lying resonance in the sequential calculation. The numerical result can be taken as a lower limit to the reaction rate, which for high temperatures can be up to about one order of magnitude above the result obtained in the sequential picture.

Summarizing, a detailed description of the triple  $\alpha$  reaction rate for temperatures beyond 3 GK requires a careful treatment of the  $2^+ \rightarrow 0_1^+$  transition. The non-resonant continuum  $2^+$  states, not included in the sequential description, are very important. For a given energy of the lowest  $2_2^+$  resonance in  $^{12}\text{C}$  below about 3 MeV, a sequential description of the process overestimates the reaction rate. For a larger resonance energy the rate of three-body calculation exceeds that of the sequential approximation due to the contribution of the non-resonant continuum states.

*Acknowledgments.* This work was partly supported by funds provided by DGI of MEC (Spain) under contract No. FIS2008-01301. One of us (R.D.) acknowledges support by a Ph.D. I3P grant from CSIC and the European Social Fund.

- 
- [1] E.E. Salpeter, *Astrophys. J.* 115, 326 (1952).
  - [2] F. Hoyle, *Astrophys. J. Suppl. Ser.* 1, 121 (1954).
  - [3] C.W. Cook, W.A. Fowler, C.C. Lauritsen, T. Lauritsen, *Phys. Rev.* 107, 508 (1957).
  - [4] M. Arnould and K. Takahashi, *Rep. Prog. Phys.* 62, 395 (1999).
  - [5] B.S. Meyer G.J. Mathews, W.M. Howard, S.E. Woosley, R.D. Hoffman, *Astrophys. J.* 399, 656 (1992).
  - [6] V.D. Efros, W. Balogh, H. Herndl, R. Hofinger, H. Oberhammer, *Z. Phys. A* 355, 101 (1996).
  - [7] M. El Eid, *Nature* 433, 117 (2005).
  - [8] H.O.U. Fynbo et al., *Nature* 433, 136 (2005).
  - [9] C. Angulo et al., *Nucl. Phys. A* 656, 3 (1999).
  - [10] P. Descouvemont and D. Baye, *Phys. Rev. C* 36, 54 (1987).
  - [11] M. Freer et al., *Phys. Rev. C* 80, 041303(R) (2009).
  - [12] R. Álvarez-Rodríguez, E. Garrido, A.S. Jensen, D.V. Fedorov, H.O.U. Fynbo, *Eur. Phys. J. A* 31, 303 (2007).
  - [13] R. de Diego, E. Garrido, D.V. Fedorov, A.S. Jensen, *Europhys. Lett.* 90, 52001 (2010).
  - [14] W. A. Fowler, G. R. Caughlan, and B. A. Zimmerman, *Annu. Rev. Astron. Astrophys.* 5, 525 (1967).
  - [15] E. Nielsen, D.V. Fedorov, A.S. Jensen, and E. Garrido, *Phys. Rep.* 347, 373 (2001).
  - [16] C. Romero-Redondo, E. Garrido, D.V. Fedorov, and A.S. Jensen, *Phys. Rev. C* 77, 054313 (2008).
  - [17] R. Álvarez-Rodríguez, A.S. Jensen, E. Garrido, D.V. Fedorov, H.O.U. Fynbo, *Phys. Rev. C* 77, 064305 (2008).
  - [18] R. de Diego, E. Garrido, D.V. Fedorov, A.S. Jensen, *Phys. Rev. C* 77, 024001 (2008).
  - [19] D.V. Fedorov, E. Garrido, A.S. Jensen, *Few-body Syst.* 33, 153 (2003).